Influence of the adatom diffusion on selective growth of GaN nanowire regular arrays

T. Gotschke,[1,2,a)] T. Schumann,[1,2] F. Limbach,[1,2] T. Stoica,[1] and R. Calarco[1,2]
[1]*Institute of Bio- and Nanosystems (IBN-1), Research Centre Jülich GmbH and JARA–Fundamentals of Future Information Technology (FIT), 52425 Jülich, Germany*
[2]*Paul-Drude-Institut für Festkörperelektronik, Hausvogteiplatz 5-7, 10117 Berlin, Germany*

(Received 23 December 2010; accepted 5 February 2011; published online 8 March 2011)

Molecular beam epitaxy (MBE) on patterned Si/AlN/Si(111) substrates was used to obtain regular arrays of uniform-size GaN nanowires (NWs). The silicon top layer has been patterned with e-beam lithography, resulting in uniform arrays of holes with different diameters (d_h) and periods (P). While the NW length is almost insensitive to the array parameters, the diameter increases significantly with d_h and P till it saturates at P values higher than 800 nm. A diffusion induced model was used to explain the experimental results with an effective diffusion length of the adatoms on the Si, estimated to be about 400 nm. © *2011 American Institute of Physics*. [doi:10.1063/1.3559618]

Recently, group III-nitride nanowires (NWs) have earned a tremendous interest in the field of nano-optoelectronics.[1,2] This material system has a direct band gap ranging by appropriate alloying from 0.7 up to 6.4 eV. Therefore, it is an ideal candidate for the realization of LEDs emitting from infrared to ultraviolet as well as high efficiency solar cells. The catalyst free molecular beam epitaxy (MBE) growth of GaN NWs on bare Si(111) was investigated by several groups,[3–9] and the capability of fabricating III-nitride NW devices using single NWs (Refs. 10–12) and NW ensembles[13,14] has been proven. However, the processes of nucleation[15–19] and diffusion of adatoms[20–23] on the NW still represent interesting and lively discussion subjects as not all the aspects have been clarified. In addition, the understanding of the growth leads to further improvements of sample quality and of the control over the structures, which in turn is beneficial for device performances. A challenge for catalyst-free MBE nitride NWs is represented by the precise NW positioning and the control on the NW sizes and density. A possible route can be found in the selective area growth (SAG) of MBE GaN NWs on patterned substrates, even though only few studies have been so far reported.[24–27] We demonstrate in this letter a method to obtain regular arrays of GaN NWs via SAG on a patterned Si mask. The study of SAG is relevant on the one hand for device applications, which require the control over the NW positioning and on the other hand for offering valuable information about the adatom kinetics of the NW growth process. Even though the NW nucleation is modified by the presence of the mask, SAG allows deeper insight into the processes of NW growth because the geometry of the NW environment during the growth is well defined in comparison with the non-selective case where a random distribution of the NW neighbors complicates the studies.

Selective growth of GaN NWs was achieved by plasma assisted MBE on patterned substrates. Si(111) substrates were cleaned by a standard *ex situ* chemical procedure and then annealed at 925 °C for 15 min for removal of the native oxide and formation of surface reconstruction. After that, the substrate temperature was reduced to 550 °C for the deposition of a thin AlN layer with a thickness of about 10 nm, using an Al beam equivalent pressure (BEP) of about 1.3×10^{-7} mbar, a plasma cell rf-power of 450 W, and nitrogen flow rate of 2.7 SCCM (SCCM denotes cubic centimeter per minute at STP). Subsequently, a Si layer of about 10 nm was deposited using a Si BEP of 1×10^{-8} mbar. The sample was then removed from the vacuum chamber and patterned by standard e-beam lithography using a polymethyl methacrylate resist. The patterns were transferred into the Si top layer by reactive ion etching whereas the underlying AlN was not affected. The mask layout contains different areas with hexagonal arrays of holes. The hole diameter and the period range from 50 nm to 120 nm and 0.3 μm to 1.5 μm, respectively. After chemical cleaning in an ultrasonic bath, the patterned substrates were annealed in the MBE chamber at 500 °C for 10 min for removal of contaminants and then heated up to 800 °C for GaN deposition. The growth of GaN NWs was performed under nitrogen rich condition using a N_2 flux of 4 SCCM with a plasma cell rf-power of 500 W and Ga BEP of 1.0×10^{-7} mbar. A Zeiss Leo1550 scanning electron microscope (SEM) was used to investigate diameter and length of the NWs as well as pattern parameters.

In Fig. 1, SEM images of GaN selective deposition on patterned Si/AlN/Si(111) with arrays of holes in the Si top layer is presented. Details about the optimization of the

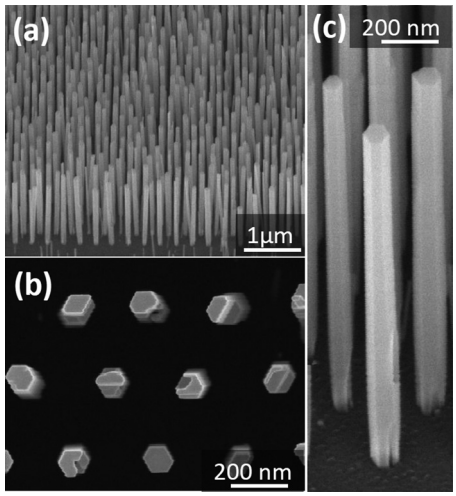

FIG. 1. SEM micrograph of SAG GaN NWs: [(a) and (c)] Bird's eye view. (b) Top view.

[a)]Electronic mail: gotschke@pdi-berlin.de.

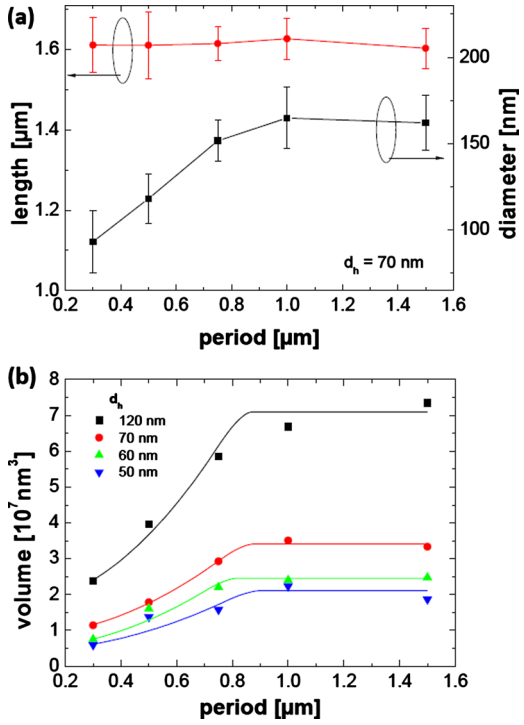

FIG. 2. (Color online) SAG GaN NWs: (a) dependence of diameter and length on P (lines are guide to the eyes); (b) measured (symbols) and calculated (lines) volume for different hole diameters with respect to P.

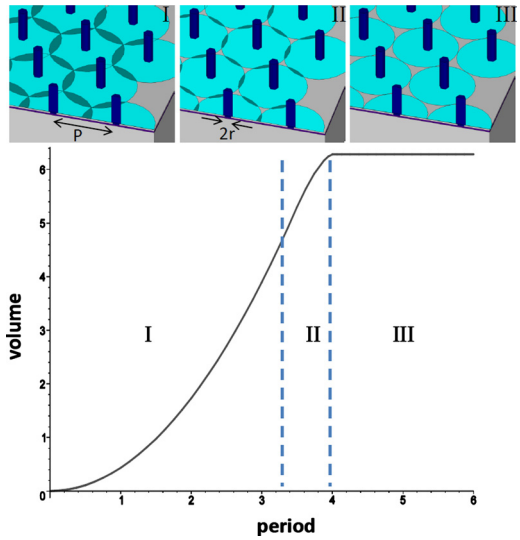

FIG. 3. (Color online) Schematic of the three different cases for the collection area in comparison with the graph of the simulated volume as a function of P in which the three cases for the collection area are depicted.

growth parameters for GaN NW selective growth using a patterned SiO_2 layer were published elsewhere.[27] The selective growth process using the Si mask was similar to that using SiO_2 as a mask material. In Fig. 1(a) we can see that the selectivity is not perfect as outside the NW arrays parasitic growth of low density NWs is still present. The parasitically grown NWs display small sizes (average diameter and length of about 30 nm and 500 nm, respectively). However, in between the arrays of selectively grown NWs the parasitic nucleation is almost suppressed [Fig. 1(b) and 1(c)]. A NW can be formed by coalescence of multiple nucleated thinner NWs. This can be inferred observing the NW base in Fig. 1(c). The coalesced NWs show steps at the top facet [Fig. 1(b)]. Nevertheless, we can see that the NWs selectively grown in the holes of the patterns are mainly oriented perpendicular to the substrate, show a clear hexagonal faceting and have homogeneous lengths and diameters.

Statistical analysis on NW sizes was performed using SEM bird's eye and top view images. The average values of the diameter and length of the NWs are plotted as a function of P in Fig. 2(a) for patterns with d_h=70 nm even though a similar behavior is observed for different d_h. The NW length is almost constant all over the entire period range (about 1.6 μm) while the diameter significantly increases before it saturates for P$>$800 nm. Moreover, the saturation occurs at about the same P value for other d_h although a significant increase of the NW diameter with d_h was observed. If we assume that during the growth the NW diameter increases from d_h to the final value we can evaluate from the data of the Fig. 2(a) a lower bound of the average radial growth rate between 0.1 and 0.4 nm/min. Comparing this with the axial growth rate estimated about 7 nm/min, the radial growth rate is more than one order of magnitude smaller than the axial growth rate; similarly to that already reported for NW growth on bare Si substrates[17] (5 nm/min and 0.15 nm/min for axial and radial growth rates, respectively). Similar length and diameter behaviors are observed as well for other material systems grown in absence of a catalyst,[28] whereas SAG in vapor-liquid-solid conditions leads to different dependences.[29,30]

The length and diameter were used to calculate the volume of the NWs assuming a cylindrical shape. The dependence of the NW volume on P for different d_h are shown in Fig. 2(b). As can be seen the volume saturates at P$>$800 nm as for the dependence of the NW diameter on P. The initial increase of the volume with P is an indication that adatoms from the area around NWs are collected and contribute to the NW growth. Thus, the value of P at which the onset of saturation is observed can be used for an empirical estimation of the effective diffusion length (L_D) of the Ga adatoms on the Si mask.

For a more quantitative evaluation we use an elementary model which takes into account the direct impinging of adatoms onto the NW and the collection of adatoms on the substrate around the NW. In fact, the area around a NW will be further named "collection area," as the adatoms collected in this area contribute to the NW growth. In more detail, the collection area can be described by a circle with the radius L_D+r (r is the NW radius) reduced by the partial overlap between nearest neighbors. We assume that every atom impinging in the area of the partial overlap diffuses to the closest NW. Therefore, only half of the area of the partial overlap accounts for the collection area. In this respect, we can identify three different cases for the collection area (see Fig. 3) as follows:

I. P is small enough, that every atom impinges in the collection area of at least one NW. Due to the hexagonal arrangement of the NWs this is true for P $\leq 3^{1/2}(L_D+r)$ resulting in a partial overlap of the collection area and therefore in a competition with the next neighbor for the impinging atoms (Fig. 3, I).

II. If P$>3^{1/2}(L_D+r)$ but still smaller than twice (L_D+r), the amount of material contributing to the NW growth is given by a circular collection area with the radius L_D+r reduced by the competition areas with the next

neighbors. It is worth to note here that in contrast to case I not the whole substrate is covered by the collection areas and consequently the collection area is dependent on L_D+r as well as P (Fig. 3, II).

III. For $P>2(L_D+r)$, no competition between the NWs takes place. Therefore, the amount of material accessible to each wire is limited by L_D resulting in a circular collection area and a constant volume of the NW independent of P (Fig. 3, III).

The volume V of a NW can be computed taking into account the contribution of the direct impinging of atoms on the NW surface (V_{di}) and that relative to the impinging flux on the collection area (A) with the following equation:

$$V = V_{di} + \omega \cdot A, \tag{1}$$

where $\omega \cdot A$ describes the effective volume of GaN originated from Ga adatoms diffusing from the substrate to the NW. ω is a proportionality factor which accounts for the NW material arising from the adatoms impinging on the substrate. Desorption and diffusion along the sidewalls are implicitly taken into account within the effective volume. If the maximal diameter of the collection area is $\gamma=2(L_D+r)$, the collection area can be expressed as a function of the period P for the three different cases as follows:

$$A = \begin{cases} \sqrt{\frac{3}{4}}P^2 - \pi r^2 & \text{(I)} \\ \frac{\pi}{4}(\gamma^2 - r^2) - \frac{3}{2}\gamma^2\left[\arccos\left(\frac{P}{\gamma}\right) - \frac{P}{\gamma}\sqrt{1-\left(\frac{P}{\gamma}\right)^2}\right] & \text{(II)} \\ \frac{\pi}{4}(\gamma^2 - r^2) & \text{(III)} \end{cases}. \tag{2}$$

In Fig. 3 we show the volume as a function of P calculated from this model and delineate the boundaries of the three cases.

It is important to note here, that all the data collected for this work originate from the same sample where the patterned areas are closely spaced in the center of the substrate and thus the NWs are subject to the same growth conditions. Moreover, V_{di} as well as ω depend only on the NW diameter and they can be consequently considered as being constant for a given d_h. In addition, the holes in the mask possess a hexagonal arrangement resulting into a constant distance between the nearest neighbors. As a consequence, in the case I the prefactor of the first term in expression (2) is that of an area of a hexagonal unit mesh. The second term accounts for the area occupied by the NW base. In the case II and III the first term describes the circular collection area reduced by the base area of the NW. In case II the partial overlap of the neighbor collection area is contained in the second term.

Combining the Eqs. (1) and (2), a good fit (solid line) of the data in Fig. 2(b) was obtained for different d_h. Furthermore, the fitted diffusion length of about 400 nm is evaluated independently on d_h. This value is comparable with that previously reported (500 nm).[24] In addition the saturation of the value of the volume at P=800 nm $[P \geq 2(L_D+r)]$ indicates that this is the distance at which the NW proximity effect vanishes.

In conclusion, we have selectively grown GaN NWs with homogeneous length of about 1600 nm and diameters within the range of 70–220 nm. The NWs exhibit hexagonal shape and a perpendicular orientation to the prepatterned substrate. Varying the period of the NW arrays, the NW diameter increases to a saturation value while the length remains constant. Based on these observations we propose a model to fit our data and to evaluate the diffusion length of adatoms on the Si substrate, which results to be about 400 nm.

The authors wish to thank K. H. Deussen for technical support. We furthermore thank R. Hey for a critical reading of the paper. This work was financially supported by the German Ministry of Education and Research project "EPHQUAM" (01BL0904).

[1] F. Qian, S. Gradecak, Y. Li, C.-Y. Wen, and C. M. Lieber, Nano Lett. **5**, 2287 (2005).
[2] T. Kuykendall, P. Ulrich, S. Aloni, and P. Yang, Nature Mater. **6**, 951 (2007).
[3] M. Yoshizawa, A. Kikuchi, N. Fujita, K. Kushi, H. Sasamoto, and K. Kishino, J. Cryst. Growth **189–190**, 138 (1998).
[4] R. Meijers, T. Richter, R. Calarco, T. Stoica, H.-P. Bochem, M. Marso, and H. Lüth, J. Cryst. Growth **289**, 381 (2006).
[5] Y. Park, S. Lee, J. Oh, C. Park, and T. Kang, J. Cryst. Growth **282**, 313 (2005).
[6] K. Bertness, N. Sanford, J. Barker, J. Schlager, A. Roshko, A. Davydov, and I. Levin, J. Electron. Mater. **35**, 576 (2006).
[7] E. Calleja, M. Sánchez-García, F. Sánchez, F. Calle, F. Naranjo, E. Muñoz, U. Jahn, and K. Ploog, Phys. Rev. B **62**, 16826 (2000).
[8] F. Furtmayr, M. Vielemeyer, M. Stutzmann, and J. Arbiol, S. Estradé, F. Peirò, J. Morante, and M. Eickhoff, J. Appl. Phys. **104**, 034309 (2008).
[9] L. Largeau, D. L. Dheeraj, M. Tchernycheva, G. E. Cirlin, and J. C. Harmand, Nanotechnology **19**, 155704 (2008).
[10] P. J. Pauzauskie and P. D. Yang, Mater. Today **9**, 36 (2006).
[11] B. Tian, T. J. Kempa, and C. M. Lieber, Chem. Soc. Rev. **38**, 16 (2009).
[12] J. Ebbecke, S. Maisch, A. Wixforth, R. Calarco, R. Meijers, M. Marso, and H. Lueth, Nanotechnology **19**, 275708 (2008).
[13] A. L. Bavencove, G. Tourbot, E. Pourgeoise, J. Garcia, P. Gilet, F. Levy, B. Andre, G. Feuillet, B. Gayral, B. Daudin, and L. S. Dang, Phys. Status Solidi A **207**, 1425 (2010).
[14] H. Sekiguchi, K. Kato, J. Tanaka, A. Kikuchi, and K. Kishino, Phys. Status Solidi A **205**, 1067 (2008).
[15] T. Stoica, E. Sutter, R. Meijers, R. Debnath, R. Calarco, H. Lüth, and D. Grützmacher, Small **4**, 751 (2008).
[16] V. Consonni, M. Knelangen, L. Geelhaar, A. Trampert, and H. Riechert, Phys. Rev. B **81**, 085310 (2010).
[17] R. Calarco, R. Meijers, R. Debnath, T. Stoica, E. Sutter, and H. Lüth, Nano Lett. **7**, 2248 (2007).
[18] O. Landré, C. Bougerol, H. Renevier, and B. Daudin, Nanotechnology **20**, 415602 (2009).
[19] J. Ristić, E. Calleja, S. Fernandez-Garrido, L. Cerutti, A. Trampert, U. Jahn, and K. H. Ploog, J. Cryst. Growth **310**, 4035 (2008).
[20] R. K. Debnath, R. Meijers, T. Richter, T. Stoica, R. Calarco, and H. Lüth, Appl. Phys. Lett. **90**, 123117 (2007).
[21] O. Landré, R. Songmuang, J. Renard, E. Bellet-Amalric, H. Renevier, and B. Daudin, Appl. Phys. Lett. **93**, 183109 (2008).
[22] R. Songmuang, O. Landré, and B. Daudin, Appl. Phys. Lett. **91**, 251902 (2007).
[23] K. A. Bertness, A. Roshko, L. M. Mansfield, T. E. Harvey, and N. A. Sanford, J. Cryst. Growth **310**, 3154 (2008).
[24] S. Ishizawa, K. Kishino, and A. Kikuchi, Appl. Phys. Express **1**, 015006 (2008).
[25] H. Sekiguchi, K. Kishino, and A. Kikuchi, Appl. Phys. Express **1**, 124002 (2008).
[26] K. A. Bertness, A. W. Sanders, D. M. Rourke, T. E. Harvey, A. Roshko, J. B. Schlager, and N. A. Sanford, Adv. Funct. Mater. **20**, 2911 (2010).
[27] T. Schumann, T. Gotschke, F. Limbach, T. Stoica, and R. Calarco, Nanotechnology **22**, 095603 (2011).
[28] S. Hertenberger, D. Rudolph, M. Bichler, J. J. Finley, G. Abstreiter, and G. Koblmüller, J. Appl. Phys. **108**, 114316 (2010).
[29] M. T. Borgström, G. Immink, B. Ketelaars, R. Algra, and E. P. A. M. Bakkers, Nat. Nanotechnol. **2**, 541 (2007).
[30] B. Bauer, A. Rudolph, M. Soda, A. Fontcuberta i Morral, J. Zweck, D. Schuh, and E. Reiger, Nanotechnology **21**, 435601 (2010).